Solving EMG-force relationship using Particle Swarm Optimization

Alberto Botter, Hamid R. Marateb, *Member, IEEE,* Babak Afsharipour, Roberto Merletti, *Senior Member, IEEE.*

***Abstract* — The Particle Swarm Optimization (PSO) algorithm is applied to the problem of "load sharing" among muscles acting on the same joint for the purpose of estimating their individual mechanical contribution based on their EMG and on the total torque. Compared to the previously tested Interior-Reflective Newton Algorithm (IRNA), PSO is more computationally demanding. The mean square error between the experimental and reconstructed torque is similar for the two algorithms. However, IRNA requires multiple initializations and tighter constraints found by trial-and-errors for the input variables to find a suitable optimum which is not the case for PSO whose initialization is random.**

I. Introduction

Most researchers agree that the torque-EMG relationship during isometric contraction of a muscle is monotonic and of the type $T_m = \omega 1_m \times sEMG^{\omega 2_m}$ where *sEMG* is the surface EMG (sEMG) envelop, *m* is the muscle index considered and $\omega 1$ and $\omega 2$ are suitable coefficients to be identified. Minimization of the mean square error, between the measured and the total estimated torque $T_t = \sum_{m=1}^{N} T_m$ (with N muscles involved) provides an estimate of the model parameters ω that in turn provide the force contributions of the individual muscles. This problem has been previously approached using the Interior-Reflective Newton Algorithm (IRNA) [1] and is addressed here using the particle-swarm-optimization (PSO) algorithm which offers some advantages.

II. Methods

A. Experimental recordings

Five healthy male subjects (mean ± std , age: 21.3 ± 2.8 years; stature 174.3 ± 2.6 cm; body mass 71.0 ± 3.4 kg) participated in the study after giving written informed consent in accordance with the Declaration of Helsinki. sEMG signals were recorded from the Biceps Brachii (BB), Brachioradialis (BR), lateral and medial head of the Triceps Brachii (TBL and TBM) during isometric voluntary flexions-extensions with the elbow flexed at 90°. A two-dimensional adhesive array of 65 electrodes of circular shape (5 columns and 13 rows, 8 mm inter-electrode distance, LISiN – Spes Medica, Battipaglia, Salerno, Italy) was used to detect signals from the BB muscle distal half. Three linear arrays of 8 electrodes (5 mm inter-electrode distance) were used to acquire signals from BR, TBL, and TBM.

The main innervation zone (IZ) was located for each muscle prior to the electrode-array placement and the adhesive arrays were placed either proximally or distally from the main IZ location depending on anatomical features of the subject. The reference electrode was placed at the wrist. The skin was abraded with a paste (Meditec–Every, Parma, Italy). Monopolar surface EMG signals were amplified (multichannel surface EMG amplifier, EMG-USB, LISiN-OT Bioelettronica, Torino, Italy), band-pass filtered (3 dB bandwidth, 10–750 Hz), and sampled at 2048 Hz with a resolution of 12 bits.

The torque signal was measured by the isometric brace used for limb fixation, amplified (Force Amplifier MISO-II, LISiN, Politecnico di Torino, Italy), sampled at 2048 Hz, displayed in real-time on a computer screen as feedback to the subjects, and recorded concurrently with the EMG signals. Three maximal voluntary isometric flexion and extension contractions (fMVC, eMVC) lasting five seconds were performed at the beginning of the experimental session, and the highest was selected as the reference MVC for each direction.

The subjects were requested to perform three series of flexion-extension force ramps lasting 25 s each. Each series consisted of four isometric ramps from n% eMVC to n% fMVC and back (with n= 30, 50, 70). Few ramps were performed before the beginning of the protocol to train the subjects to track the ramp target on the biofeedback screen.

Monopolar sEMG signals were digitally band-pass filtered (20-450 Hz, 4th order Butterworth filter) and the force signal was low-pass filtered with a cut-off frequency of 1 Hz (4th order non-causal Butterworth filter). Single differential (SD) and double differential (DD) signals were computed along the fiber direction, thus obtaining three sets of signals (monopolar, SD, and DD). The envelope of sEMG signals was extracted by non-causal digital low-pass filtering (1 Hz, 4th order Butterworth filter) of the rectified signals. For each muscle (i.e. detection system) the global envelope was computed as the spatial average of the corresponding recorded signals.

B. The Mathematical model

In this work, the estimated torque acting on the elbow is described by Eq.1.

(1)

Where is the n-th sample of the envelope ($sEMG_m$) (V), is the estimated torque (Nm), *muscles* identify the set of muscles considered. In this model, $\omega 1_m$ is the linear weight associated with the muscle *m*, and $\omega 2_m$ is the exponential weight that takes into account the non-linearity

Manuscript received March 25, 2011. This work was supported by Compagnia di San Paolo and Fondazione CRT.

A. Botter, H.R. Marateb, B. Afsharipour, R. Merletti are with the Laboratory for Engineering of the Neuromuscular System (LISiN), Department of Electronics, Politecnico di Torino, Torino, Italy (e-mail: roberto.merletti@polito.it).

of the relationship between sEMG and torque of muscle *m*. To estimate the model parameters ($\omega 1_m$, $\omega 2_m$), the sEMG-torque relationship can be formulated as an optimization problem by minimization of the objective function defined in Eq.2,

$$e = \sum_{n=1}^{K} \left(M[n] - \tilde{M}[n] \right)^2 \quad (2)$$

where $M[n]$ is the measured torque, $\tilde{M}[n]$ is the estimated torque (Eq.1), *n* is the sample index, and *K* is the number of samples in the signal.

C. Constraint Optimization

The values of the linear weights $\omega 1_m$ resulting from the training phase are expected to be positive for flexor muscles and negative for extensor muscles. The values of $\omega 2_m$ are expected to be in the range (0,1] [2],[3],[4].

The objective function customized for our study is reported in Eq.3. The constraint optimization is formulated using helping variables to find $\omega 1_m$ and $\omega 2_m$.

$$e = \frac{\sum_{n=1}^{K_t} \left(M[n] - \sum_{m=1}^{4} z_m \times |x_m| \times sEMG_m[n]^{\left|\frac{y_m}{R}\right|} \right)^2}{\sum_{n=1}^{K_t} (M[n])^2} \quad (3)$$

Where helping variables x_m and y_m are real numbers ranging within [-R,R] (R=100, in our study), the first and second muscles are the elbow flexors (m=1,2; z_m=1: biceps brachii, and brachioradialis) while the third and forth muscles are elbow extensors (m=3,4; z_m=-1: the medial and lateral heads of triceps brachii). Twenty five seconds (the first cycle of flexion-extension) were used to estimate the linear and exponential weights. K_t is the number of samples corresponding to the first cycle of flexion-extension.

The accuracy of the algorithm was assessed in terms of relative errors (in percent), defined as $100 \times \sqrt{e}$.

The performance of the algorithm was measured using Evals, number of evaluations of the objective function and the total execution time of the algorithm used to solve the optimization problem.

D. Particle Swarm Optimization (PSO)

PSO is a meta-heuristic population-based stochastic optimization algorithm, originally proposed to simulate the social behavior of a flock of birds [5]. In this method, each "particle" is a candidate solution that "flies" through the search space. The path of each particle is influenced by its own experience and that of its neighbors. In our case, the neighborhood of each particle is the entire swarm (star topology) [6]. Each particle (*i*) is characterized by: its current position ($\mathbf{x_i}$); its current velocity ($\mathbf{v_i}$); the personal best position it has found (corresponding to the lowest minimum of the cost function so far) ($\mathbf{y_i}$); the best position reached by any of the particles so far ( ).

At each iteration, these features are updated as follows [7]:

$$\mathbf{v}_i^j = w\mathbf{v}_i^{j-1} + c_1\mathbf{r}_1 \bullet \left(\mathbf{y}_i^j - \mathbf{x}_i^j \right) + c_2\mathbf{r}_2 \bullet \left(\hat{\mathbf{y}}^j - \mathbf{x}_i^j \right) \quad (5)$$

where *j* is the iteration number, and • denotes element-by-element multiplication. The new velocity depends on the previous velocity and on the distances of the particle from the personal and neighborhood best positions [6], with the coefficient ***w*** being the "inertia" weight, c_1 the "cognitive acceleration" coefficient (=2.0), c_2 the "social acceleration" coefficient (=0.5), and $\mathbf{r_1}$ and $\mathbf{r_2}$ random vectors whose elements are uniformly distributed in U(0,1). A large value of inertia weight favors global search ("exploration"), while a small value favors local search ("exploitation"). A strategy is to set the value high initially (1.2) to encourage exploration, and then reduce it towards a low value (0.1) to fine tune the final solution. To prevent oscillations the velocity components are limited to $[-v_{max}, v_{max}]$, where v_{max} is set to 4. Whenever the absolute value of the positions **x** reaches the limit 100, they are clamped and the sign of the corresponding velocities **v** is changed to continue searching within the defined ranges. The maximum number of iterations (max_iter) is 500×K+200, where K is the number of muscles. The number of particles in the swarm is set to $20+10\sqrt{2*K}$ .Several extensions and modifications to the standard method were used to speed convergence and discourage premature convergence to a non-global minimum as follows:

(1) Multi-start PSO Approach: the PSO algorithm is run twice [8]. The best result found at the first iteration is used as a particle in the second run. Increasing the number of runs increases the chances of finding the global minimum, but at the cost of increased computation time. (2) Sobol's quasirandom sequence: sixty percent of the particles are filled with uniform random values, while the remaining 40% are filled with Sobol's quasirandom sequence [9], which covers the search space regularly. (3) Random PSO Approach: Randomized particles are introduced in the swarm as follows [8]: every 40 iterations, the positions of the particles filled with the Sobolian Sequence, are re-initialized using the next generation of Sobol's sequence. (4) Breeding Algorithm: breeding (arithmetic cross-over) operator was taken from the genetic algorithm to increase the performance of the PSO [10]. Every iteration, there is a 20% chance that two offspring particles are generated using the arithmetic mean of two randomly chosen (from the non-Sobolian partition) parent particles. (5) Swarm Regeneration and Multi-Swarm Strategy [11]: if a swarm's best solution does not change for 200 iterations, then a new, randomly initialized swarm is created to increase the exploration while the original swarm is kept for further tuning the solution found. The maximum number of Swarms is set to the number of muscles. After the initialization of PSO, two swarms are generated. A swarm is deleted if all of its particles converge to a single solution. Finally, a multi-criteria for terminating the PSO (based on the maximum number of iterations and the diameter of the swarm) was used [12].

(4)

TABLE I

RESULT OF PARTICLE SWARM OPTIMIZATION ON SINGLE-DIFFERENTIAL RECODING FOR FIVE SUBJECTS DURING ELBOW FLEXION-EXTENSION ISOMETRIC RAMPS ON THE TRAINING AND TEST SETS @ 30%, 50% AND 70% MAXIMUM VOLUNTARY CONTRACTIONS (MVC); AVERAGE (±SD) REL ERR OBTAINED IN THE TRAINING AND TEST SETS WERE 10.2±3.5 (%) AND 14.4±4.5 (%) RESPECTIVELY.

Subjects			S1	S2	S3	S4	S5
30% MVC	Training Set	# Swarms	2 , 4	4 , 4	2 , 4	-	2 , 4
		Evals	0.80	1.08	0.80	-	0.80
		Time (s)	465	619	460	-	478
		Rel Err (%)	10.8	7.4	14.3	-	18.6
	Test Set	Rel Err (%)	14.6	10.6	13.9	-	22.2
50% MVC	Training Set	# Swarms	3 , 4	2 , 4	2 , 4	2 , 4	4 , 4
		Evals	1.92	0.80	0.80	0.80	0.97
		Time (s)	1121	461	475	508	595
		Rel Err (%)	9.5	6.6	6.6	10.1	10.7
	Test Set	Rel Err (%)	12.3	10.3	11.1	11.4	24.0
70% MVC	Training Set	# Swarms	2 , 4	-	4 , 3	-	2 , 4
		Evals	0.80	-	1.52	-	1.58
		Time (s)	467	-	956	-	979
		Rel Err (%)	11.8	-	7.6	-	6.5
	Test Set	Rel Err (%)	14.7	-	16.4	-	11.3

Swarms=number of swarms generated in the PSO algorithm for the first and second runs respectively, Evals= number of evaluations of the objective function (x10^6), Time= total execution time of the PSO at the first and second runs, Rel Err= the RMS of the force prediction error divided by the RMS of the measured force.

TABLE II

THE CROSS-CHECKING RESULTS OF PARTICLE SWARM OPTIMIZATION ON MONOPOLAR AND SINGLE-DIFFERENTIAL RECORDINGS FOR 5 SUBJECTS DURING ELBOW FLEXION-EXTENSION ISOMETRIC RAMPS ON THE TRAINING AND TEST SETS (USING THE COEFFICIENTS OBTAINED @ 50% MVC TO ESTIMATE THE FORCE @ 30% AND 70% MVC)

Subjects			S1	S2	S3	S4	S5	Total: Mean ± Std
Monopolar	Rel Err (%)	30% MVC	33.6	19.4	32.3	-	17.9	26.0 ± 7.2 N=7
		70% MVC	18.2	-	31.4	-	29.2	
Single-Differential	Rel Err (%)	30% MVC	23.8	13.7	21.9	-	35.1	25.3 ± 6.7 N=7
		70% MVC	28.1	-	26.1	-	28.4	
Double-Differential	Rel Err (%)	30% MVC	29.7	16.4	15.2	-	42.2	28.7 ± 10.0 N=7
		70% MVC	37.0	-	30.9	-	29.5	

Rel Err= the RMS of the force prediction error (using the coefficients obtained @ 50% MVC) divided by the RMS of the measured force.

III. RESULTS

Fig. 1a shows the comparison between the recorded and estimated torques. The contribution of the four muscles acting on the elbow joint is also reported. Fig. 1b depicts the single differential sEMG envelops of the above mentioned muscles. Table I reports the results of Particle Swarm Optimization on Single-Differential Recoding for 5 subjects during elbow flexion-extension isometric ramps on the training and test sets at 30%, 50% and 70% Maximum Voluntary Contractions (MVC). The cross-checking results of Particle Swarm Optimization on Monopolar, Single-Differential, and Double Differential recordings for elbow flexion-extension at 30% and 70% MVC are reported in Table II. The missing data in the tables correspond with the conditions in which subjects could not follow the force target and the force variations were not acceptable.

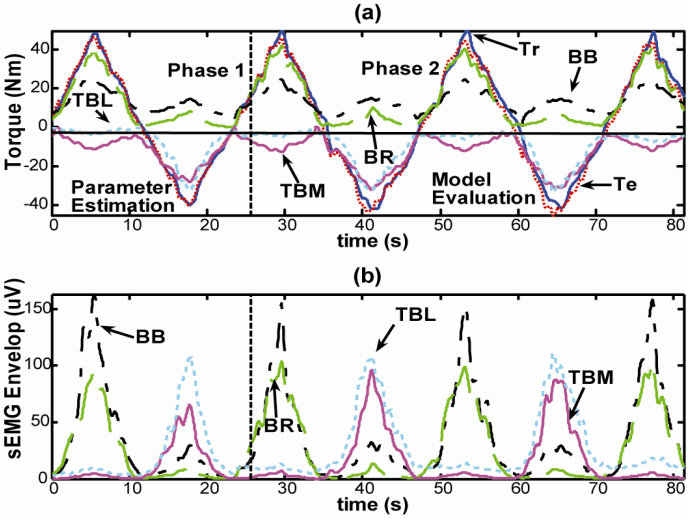

Fig. 1. a) recorded Torque "Tr" (solid blue) and estimated Torque "Te" (dotted red) in addition to the reconstructed Torques for each muscle (top). b) single differential sEMG envelopes for biceps brachii (dashdot black), brachioradialis (dashed green), medial and lateral heads of the triceps brachii (solid magenta and dotted cyan) for subject no. 5 during a 70 %MVC elbow flexion-extension isometric ramps. The sEMG signals and measured torque up to 25.6 s (shown by the tick dashed black line) were used to estimate the parameters (phase 1) and the rest was used for the test (phase 2).

IV. DISCUSSION AND CONCLUSIONS

The issue of muscle force prediction from EMG has been addressed in the literature, e.g. [13], [14], [15]. Unlike other methods that considered linear relationship between EMG and force [13], [14], a non-linear model was proposed in this work. As underlined by Clancy et al. [13], using non-linear models is possible to capture additional subtle behavior in EMG-force relationship. Also, our model does not require preset musculoskeletal parameters (e.g. parallel elastic stiffness and damping [15]).

When solving an optimization problem, the goal is to find the global optimal solution in an acceptable amount of time. There are different methods capable of finding solutions to optimization problems including exact methods, Heuristics and Meta heuristics [16]. Exact methods solve optimization problems by searching the entire solution space exhaustively. However, a large number of optimization problems belong to the NP-complete class and solutions cannot be found by exact methods except for small instances. For example, in our case the objective function has 8 continuous input parameters; using the absolute input ranges of 10 for linear coefficients (in steps of 0.1) and 1 for exponential ones (in steps of 0.01), more than 1.45×10^{20} cases should be taken into account to find the global optimum by brute-force approach. This is quite time-consuming and impractical. Also, its accuracy depends on the resolution (step) chosen for each input variable.

Approximation methods in optimization, on the other hand, provide the approximate solution in reasonable amount of time but imply the risk of not finding the global optimum. In Heuristics, e.g. local search, the best possible solution is found close to the starting point. Local search does not guarantee the finding of the best solution; it is only able to find the best one in the neighborhood of the starting point. Thus, it is quite probable to get stuck in the local optimum.

Evolutionary Computations (EC) simulates some of the known mechanisms of evolution. They differ from the traditional search methods in the following three concepts: they use a population of potential solutions, decision making processes are guided by fitness information alone and decisions are probabilistic rather than deterministic. In EC, the possibility of getting stuck in local optimum is decreased by introducing a population of possible solutions (particles) and the randomness of their behavior. A particle by itself has almost no power to solve any problem; progress occurs when the particles interact [17]. PSO is one of the recent EC techniques introduced and its application has increased exponentially in the last decade [17]. Using multiple swarms, it was possible to keep track of some of the local minimums found by the swarms before re-generation that helps to consider other minimum points that are more physiologically feasible.

With respect to previously tested methods [1], the PSO algorithm eliminates the problems of initialization and has an intrinsically higher likelihood of finding the global minimum and nearby relative minima that might be worth of consideration. However, the computational load of PSO is greater than that of IRNA. The fact that the EMG of some deep muscles cannot be collected with surface electrodes (e.g. brachialis muscle) remains a strong limitation and major cause of error. The error in reconstructing the total torque with the two algorithms is not that different (13.2 ± 3 % for IRNA, and 10.2 ± 4 % for PSO in the training set). However, IRNA required several initializations and tighter constraints found by trial-and-errors for the input variables to find a suitable optimum which was not the case for PSO whose initialization was random.

Future works will focus on the validation of PSO results by simulation (using a joint model), and on designing a multi-objective optimization to include other cost functions e.g. minimizing the energy consumed in our muscles as the optimum control of our neuro-muscular system and implementing the PSO in C++, with multi-threads (each swarm as a thread) and using the Vectorization packages [7] to reduce the computational time listed in Table I.

In this work the activity of the muscles was estimated by spatial averaging of the sEMG envelop over the entire detection system. Automatic segmentation of multichannel EMG activity to improve the estimation of neuromuscular activity [18] and other pre-processing techniques (such as whitening [19]) might increase the performance of the algorithm. Moreover, our results must be compared with those obtained in similar studies [13], [14].

ACKNOWLEDGMENTS

The authors are grateful to M. Aventaggiato for collecting and providing the experimental data and Dr. M.A. Minetto for fruitful discussions. This work was supported by Compagnia di San Paolo and Fondazione CRT.

REFERENCES

[1] R. Merletti, M. Aventaggiato, “Emg-Force Relationship: Preliminary Data On Load Sharing,” XVIII Congress of the International Society of Electrophysiology and Kinesiology. Aalborg, Denmark, 16-19 June 2010. ISBN: 978-87-7094-047-4.

[2] J.H. Lawrence, C.J. De Luca, “Myoelectric signal versus force relationship in different human muscles,” Journal of Applied Physiology, Vol. 54, No. 6, pp.1653 – 1659, 1983.

[3] P.J. Sparto PJ, et. al., “Effect of electromyogram-force relationships and method of gain estimation on the predictions of an electromyogram-driven model of spinal loading,” Spine, Vol. 23, No. 4, pp.423 – 429, 1998.

[4] H.P. Clamann, “Motor unit recruitment and the gradation of muscle force,” Physical Therapy, vol. 73, No. 12, pp.830 - 843, 1993.

[5] J. Kennedy, R. C. Eberhart, Y. Shi, “Swarm Intelligence,” Morgan Kaufman Publishers, Academic Press, 2001. ISBN: 1-55800-505-9.

[6] F. Van den Bergh, A. P. Engelbrecht, “A study of particle swarm optimization particle trajectories,” Information Sciences, vol. 176, pp. 937-971, 2006.

[7] H.R. Marateb, K.C. McGill, “Resolving superimposed MUAPs using particle swarm optimization,” IEEE Trans Biomed Eng., Vol. 56, No.3, pp. 916-9, 2009.

[8] F. Van Den Bergh, “An analysis of particle swarm optimizers,” PhD thesis, University of Pretoria, 2001, pp.118-122.

[9] B. Fox, “Algorithm 647: Implementation and relative efficiency of quasi-random sequence generators," ACM Trans. Math. Software, vol. 12, pp. 362–376, 1986.

[10] T. Krink and M. Lovbjerg, “The LifeCycle model: Combining particle swarm optimization , genetic algorithms and hill climbers,” In Lecture Notes in Computer Science: Proceedings of Parallel Problem Solving from Nature VII, Springer, vol. 2439, pp.621-630, 2002.

[11] K. E. Parsopoulos and M. N. Vrahatis, “Modification of the particle swarm optimizer for locating all the global minima,” In V. Kurkova, N. Steele, R. Neruda, M. Karny (Eds.), Artificial Neural Networks and Genetic Algorithms, Springer, pp. 324–327, 2001.

[12] K. Zielinski , R. Laur, “Stopping Criteria for a Constrained Single-Objective Particle Swarm Optimization Algorithm,” Informatica, Vol.31 ,pp.51–59,2007.

[13] E.A. Clancy, O. Bida, D. Rancourt, “Influence of advanced electromyogram (EMG) amplitude processors on EMG-to-torque estimation during constant-posture, force-varying contractions,” J Biomech. Vol. 39, No. 14, pp.2690-8, 2006.

[14] M.J. Hoozemans, J.H. van Dieën, “Prediction of handgrip forces using surface EMG of forearm muscles,” J Electromyogr Kinesiol. Vol. 15, No. 4, pp.358-66, 2005.

[15] L.L. Menegaldo, L.F. de Oliveira, “Effect of muscle model parameter scaling for isometric plantar flexion torque prediction,” J Biomech. Vol. 42, No. 15, pp.2597-601, 2009.

[16] R. Mendes, “Population Topologies and Their Influence in Particle Swarm Performance,” PhD dissertation, Departamento de Informática Escola de Engenharia Universidade do Minho, University of Pretoria, April 21, 2004, p.14.

[17] R. Poli, J. Kennedy, T. Blackwell, “Particle swarm optimization: an overview,” Swarm Intell., Vol. 1, pp.33-57, 2007.

[18] T.M. Vieira, R. Merletti, L. Mesin, “Automatic segmentation of surface EMG images: Improving the estimation of neuromuscular activity,” J Biomech. Vol. 10, No. 43, pp. 2149-58, 2010.

[19] E.A. Clancy, N. Hogan, “Relating agonist-antagonist electromyograms to joint torque during isometric, quasi-isotonic, nonfatiguing contractions,” IEEE Trans Biomed Eng. Vol. 44, pp. 1024-8, 1997.